Influence of aerosol formation mechanism by an ultrasonic field on particle size distribution of ceramic powders

V. Jokanović [a], Dj. Janaćković [b,*], D. Uskoković [c]

[a] *Institute for Technology of Nuclear and Other Mineral Row Materials, Franchet d'espere 86, 11 000 Belgrade, Yugoslavia*
[b] *Faculty of Technology and Metallurgy, Kamegijeva 4, 11 000 Belgrade, Yugoslavia*
[c] *Institute of Technical Sciences of the Serbian Academy of Sciences and Arts, Knez Mihajlova 34, 11 000 Belgrade, Yugoslavia*

Abstract

Aerosol droplet genesis by ultrasonic atomization has been theoretically studied using a model for three-dimensional spherical/ellipsoidal waves generated by excitation of a system of given geometry by forced frequency of an ultrasonic oscillator. Analyzing the harmonic function of the rate potential, an equation has been derived that defines the mean diameter and the distribution spectrum of aerosol droplets formed at the surface of a liquid. Comparison has been made between the calculated values for the mean particle sizes and their distribution with those obtained experimentally for Al_2O_3, mullite and cordierite powders synthesized from different precursors. © 1999 Elsevier Science B.V. All rights reserved.

Keywords: Aerosol formation mechanism; Ceramic powder; Particle size distribution; Ultrasonic field

1. Introduction

Use of ultrasound in sonochemistry is a specific modern technique for obtaining amorphous and nano-materials [1], especially amorphous metals from organo-metallic compounds with pronounced volatile properties (metal carbonyls or nitrosyls). Small clusters of metal atoms (nanometers in size) can be obtained, for instance, by ultrasonic excitation and changes produced by it inside the given metal complex (sonoluminescence). Such materials exhibit exceptional catalytic, or in the case of ferromagnetics, magnetic properties (supermagnetics, without hysteresis). Also, ultrasonic excitation (ultrasonic atomization) combined with subsequent reduction or exposure of the system to a specific carrier gas atmosphere can give different non-oxide (carbides, nitrides, etc.) and composite materials (Al_2O_3–Pt, ZrO_2–Pt) with well-defined particle geometry.

Owing to great similarity between the morphological and structural characteristics of powder particles obtained by ultrasonic atomization and subsequent thermal treatment consisting of precipitation, drying, pyroly-sis and sintering [2–7], special attention has been focused in this paper on powder particle genesis. The formation of particles has been considered as a process of harmoni-zation of the physical field of the ultrasonic oscillator with that of the given system during aerosol droplets genesis. This process is especially significant because through it the identity of the system is established, which during transformation under thermal treatment gives the final form to the so-defined starting structure.

In this paper a new approach and model for predic-tion of the particle size distributions produced by ultra-sonic spray pyrolysis are presented.

The model of formation of aerosol droplets in the given ultrasonic field arose from the theoretical model of three-dimensional spherical/ellipsoidal capillary waves and the process of harmonization of the forced field of an ultrasonic generator with the field of frequen-cies characteristic of the system.

An analysis was made based on a comparison of the equation derived for calculation of the mean particle size with Lang's equation [2]. Also, experimentally determined and theoretically estimated particle size distribution spectra for a series of selected systems (Al_2O_3, mullite, cordierite) [8–11], obtained from different precursors, were compared and a very good agreement between them was found. The process of genesis considered at the phenomenon level, is an inter-action between outer and inner physical fields, which

* Corresponding author. Fax: +381 11-3370-387.
E-mail address: nht@elab.tmf.bg.ac.yu (Dj. Janaćković)

Nomenclature

p	internal pressure in the liquid	d_n	discrete value in distribution spectrum
p_o	gas-phase pressure outside the liquid	f_{no}	minimal frequency in spectrum standing waves
σ	surface liquid tension		
ζ	amplitude of the surface standing wave	d_p	particle size diameter
ϕ	rate potential	d	aerosol droplet diameter
y	amplitude of the standing wave in the y-axis direction	ρ_o	oxide density
		M_o	oxide molecular mass
h	liquid column depth	M_s	starting precursor molecular mass
k	wave number	C_p	precursor concentration
t	time	Y_p	resonant wave amplitude
x, y, z	coordinates	H	forced force
$y\,e^{ikh}$	factor of amplitude amplification	β	factor of environment resistance
g	inertial force	m_o	oscillator mass
d	diameter of an aerosol droplet	Δf	difference between forced frequency of ultrasonic oscillator and the characteristic frequency of liquid column
R_1, R_2	minimal and maximal radius sphere deformed standing waves		
θ, ϵ	angles in polar coordinates	Q	quality factor
$Y_{lm'}(\theta, \epsilon)$	spherical Laplace's function	f_s	characteristic frequency of liquid column
$P_l^{m'}(\cos\theta)$	Legendere's function		
l, m'	integers in Legendere's function	i	imaginary unit
ω	spherical frequency of ultrasonic wave oscillation	η	viscosity coefficient
		A, B	harmonization constants
q, r, s	characteristic dimension parameters of standing wave function	$p(\tau)$	periodical function dependent on time
a, b, h	dimensions of the liquid column	τ	time
m, n, p	selected values of degenerated wave frequency integers	μ	amplification exponent of standing wave
ω_s	spherical oscillation frequency	$y(\tau)$	wave amplitude
c	rate of capillary wave propagation	ϕ_x, ϕ_y	rate potential in x and y directions

can be used to explain and quantify various phenomena [12,13].

2. Experimental

For the synthesis of alumina powders, 0.5 M aqueous solutions of $AlCl_3 \cdot 6H_2O$ (for the A-1 powder) and $Al(NO_3)_2 \cdot 9H_2O$ (for the A-2 powder) were used as precursors.

For the synthesis of mullite (M-2 and M-3) powders, three starting 0.025 M solutions were prepared.

- M-2 sample: $Al(NO_3)_3 \cdot 9H_2O$ was dissolved in an aqueous solution of silicic acid ($T = 20°C$, pH = 2.5, particle diameter below 2 nm).
- M-3 sample: TEOS previously dissolved in ethanol was added to an aqueous solution of $Al(NO_3)_3 \cdot 9H_2O$ ($T = 80°C$, pH = 1) with added HNO_3 (as a catalyst for TEOS hydrolysis), in the ratio TEOS:ethanol:water = 1:2:17 (such a high TEOS:water ratio was used owing to difficult atomization of alcohol solutions). In this way, TEOS was completely hydrolyzed to form silicic acid.

For the synthesis of cordierite (C-1) powder, a 0.01 M solution was prepared by dissolving $MgCl_2 \cdot 6H_2O$ and $Al(NO_3)_3 \cdot 9H_2O$ in a 3 wt% aqueous solution of silicic acid with pH = 2.8.

The solution atomization was carried out with an ultrasonic GAPUSOL-RBI-9001 atomizer at a resonant frequency of 2.5 MHz and a capacity of 400 cm³/h, generating aerosol droplets of a mean diameter of 2 μm.

Aerosol droplets were then inserted into an air stream at a flow rate of 30–40 dm³/h, in a 1 m long furnace, at 900°C. The residence time of droplets/particles inside the furnace was 95 s, assuming the air flow rate and droplet velocities to be equal. The heating rate of droplets/particles was 18°C/s. A schematic diagram of the apparatus for powder synthesis was given earlier [8–11].

Characterization of the powders obtained was made by SEM (JEOL-JSM-5300), TEM (JEOL-JSM-100) and quantitative stereological analysis (VIDEO PLAN, KONTRON semi-automatic video analyzer) immediately after atomization and subsequent heating up to 1300°C.

Quantitative stereological analysis data on mean

powder particle size and particle size distribution spectra, being extremely important for the genesis of powders, were especially considered from the point of view of distribution characterization and data comparison (experimental with calculated values).

3. Theoretical model

The forced frequency of an ultrasonic oscillator causes the generation of equivalent oscillations inside the given liquid column, i.e. transversal (perpendicular to the ultrasonic oscillator plane) and longitudinal (parallel to the ultrasonic oscillator plane) wave degeneration (Fig. 1). The shape of the spatial waves formed depends on the superposition conditions determined by the following parameters: surface tension, liquid viscosity, vessel geometry (liquid column depth and vessel shape), and forced ultrasonic oscillator frequency.

In a general case the waves are ellipsoidal and their excenters depend on the ratio of the damping factors of the transverse to longitudinal waves.

For sufficiently low values of the liquid column depth, the waves induced have a spherical shape (the damping factor for transverse waves can be compared with that for longitudinal waves that propagate the lamellar boundary layers of the liquid with almost negligible resistance).

For the simplest case of spherical wave generation assuming the internal pressure in the liquid p to be much greater than the gas-phase pressure outside the liquid p_o, according to the Laplace law it follows that

$$p \approx p - p_o = \sigma \left(\frac{\partial^2 \xi}{\partial x^2} \right) \tag{1}$$

where σ is the surface liquid tension, and $\xi(x, y)$ is the amplitude of the surface standing wave formed.

Based on Bernoulli's equation [8,14]

$$p = \rho \frac{d\phi}{dt} - gy \tag{2}$$

where ρ is the liquid density, g is the inertial force acting on the liquid in contact with an ultrasonic oscillator,
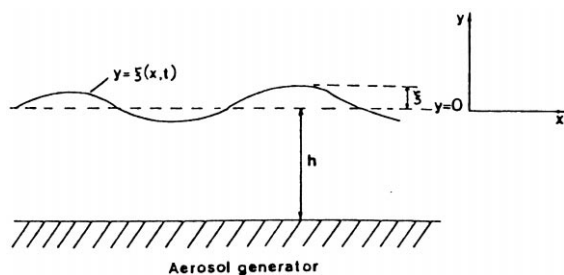

Fig. 1. The wave at the surface of a liquid column induced by an ultrasonic wave generator (presented in the x–y plane).

and y is the amplitude of the wave in the y-axis direction ($y = \xi$), and the condition is fulfilled that:

$$\frac{\partial \xi}{\partial t} = - \frac{\partial \phi}{\partial y} \tag{3}$$

where ϕ is the rate potential.

Then assuming that the change in aerosol droplet velocity is dominant in relation to the difference in velocities of two aerosol droplets present at the same time and equal distance from the equilibrium, that is

$$\frac{\partial \phi}{\partial t} \gg - \frac{\partial \phi}{\partial x} ; \frac{\partial \phi}{\partial y} . \tag{4}$$

From the condition

$$\nabla^2 \phi = 0 \tag{5}$$

for $h \leq y < \xi + h$, it follows that

$$\frac{\partial \phi}{\partial t} + gy = - \frac{\sigma}{\rho} \frac{\partial^2 \xi}{\partial x^2} \tag{6}$$

where h is the liquid column depth.

Assuming $h \gg y$, the rate potential can be written in the form

$$\phi = - \frac{1}{k} \frac{dy}{dt} \operatorname{ch}(kh) \tag{7}$$

where k is the wave number, and dy/dt is the factor of the wave amplitude change with time.

Knowing that the amplitude can be defined as a hyperbolic periodic function in the form

$$\xi = y \, e^{ikh} \operatorname{sh}(kh) \tag{8}$$

where $y \, e^{ikh}$ is the factor of amplitude amplification, then from Eq. (6), for $y = \xi$, it follows that

$$\frac{d^2 y}{dt^2} + \left[\frac{\sigma}{\rho} k^3 \operatorname{th}(kh) + kg \operatorname{th}(kh) \right] y = 0 \tag{9}$$

because

$$\frac{\partial \phi}{\partial t} = \frac{1}{k} \frac{d^2 y}{dt^2} \operatorname{ch}(kh) \, e^{ikh} \tag{10}$$

and

$$\frac{\partial^2 \xi}{\partial x^2} = k^2 y \, e^{ikh} \operatorname{sh}(kh). \tag{11}$$

The given type of Eq. (9) presents a typical form of the so-called Mathieu functions [15], the solution of which under the condition

$$d = \frac{\pi}{k} \tag{12}$$

where d is the diameter of an aerosol droplet, using

Floquet's theorem [15–17], gives

$$d = \left(\frac{\pi\sigma}{\rho f^2} \right)^{1/3} \tag{13}$$

where f is the frequency of ultrasonic oscillator.

Assuming that the degeneration in shape of spatial standing waves (sphere deformation between R_1 and R_2) is caused by the difference in damping factors of the transverse and longitudinal waves, we get

$$\rho \frac{\mathrm{d}\phi}{\mathrm{d}t} + p_o = -\sigma \left(\frac{1}{R_1} + \frac{1}{R_2} \right) \tag{14}$$

whereby

$$\frac{1}{R_1} + \frac{1}{R_2} = \frac{2}{R} - \frac{2\xi}{R^2} - \frac{1}{R^2} \left[\frac{1}{\sin^2\theta} \frac{\partial^2\xi}{\partial\epsilon^2} \right.$$
$$\left. + \frac{1}{\sin\theta} \frac{\partial\left(\sin\theta \frac{\partial\xi}{\partial\epsilon} \right)}{\partial\theta} \right] \tag{15}$$

where R is the mean radius of spatial standing waves; ϵ and θ are the corresponding angles when the system transits into polar coordinates [14,18].

If the rate potential is assumed to satisfy the Laplace equation

$$\Delta\phi = 0 \quad \text{and} \quad \nabla^2\phi = 0 \tag{16}$$

then

$$\rho \frac{\mathrm{d}\phi}{\mathrm{d}t} + \sigma \left\{ \frac{2}{R} - \frac{2\xi}{R^2} - \frac{1}{R^2} \left[\frac{1}{\sin\theta} \frac{\partial\left(\sin\theta \frac{\partial\xi}{\partial\epsilon} \right)}{\partial\theta} \right. \right.$$
$$\left. \left. + \frac{1}{\sin^2\theta} \frac{\partial^2\xi}{\partial\epsilon^2} \right] \right\} + p_o = 0. \tag{17}$$

Further, assuming that

$$\frac{\partial\xi}{\partial t} = \frac{\partial\phi}{\partial r} \tag{18}$$

we get

$$\rho \frac{\partial^2\phi}{\partial t^2} \bigg|_{r=R} - \frac{\sigma}{R^2} \left\{ 2\frac{\partial\phi}{\partial r} + \frac{\partial}{\partial r} \left[\frac{1}{\sin\theta} \frac{\partial\left(\sin\theta \frac{\partial\phi}{\partial\theta} \right)}{\partial\theta} \right. \right.$$
$$\left. \left. + \frac{1}{\sin^2\theta} \frac{\partial^2\phi}{\partial\epsilon^2} \right] \right\}_{r=R} = 0. \tag{19}$$

The solution of the given equation in the form of a spatial standing wave gives the following function

[17,18]:

$$\phi = e^{-i\omega t} f(r, \theta, \epsilon) \tag{20}$$

where the function of polar coordinates $f(r, \theta, \epsilon)$ satisfies Laplace's equation.

The solution of Laplace's equation can be presented as a linear combination of so-called spherical volume functions:

$$F_{kj} = r^l Y_{lm'}(\theta, \epsilon) \tag{21}$$

where $Y_{lm'}(\theta, \epsilon)$ is the spherical Laplace function which can be presented by

$$Y_{lm'}(\theta, \epsilon) = P_l^{m'}(\cos\theta)\, e^{im'\epsilon} \tag{22}$$

where $P_l^{m'}(\cos\theta)$ is Legendre's function, which can be expanded to Legendre's polynomial of order l, where l can be an integer from 0 to 1, and m for the given l is

$$m' = 0, \pm 1, +2, \ldots, \pm l. \tag{23}$$

The partial solution of Eq. (20) can be written as

$$\phi = A\, e^{-i\omega t} r^l P_l^{m'}(\cos\theta)\, e^{im'\epsilon}. \tag{24}$$

Since the spherical function $Y_{lm'}$ satisfies the equation

$$\frac{1}{\sin\theta} \frac{\partial\left(\sin\theta \frac{\partial Y_{lm'}}{\partial\theta} \right)}{\partial\theta} + \frac{1}{\sin^2\theta} \frac{\partial^2 Y_{lm'}}{\partial^2\epsilon} + l(l+1)Y_{lm'} = 0 \tag{25}$$

the solution of Eq. (19) can be obtained in the form

$$\rho\omega^2 + \frac{l\sigma}{R^3}[2 - l(l+1)] = 0 \tag{26}$$

where ω is the spherical frequency of ultrasonic wave oscillation.

The minimum value of the equation solution that has a physical meaning can be obtained for $l = 2$, since $\omega = 2\pi f$ is in the form

$$d_{\min} = 2\frac{\sqrt[3]{2}}{\pi} \left(\frac{\sigma\pi}{\rho f^2} \right)^{1/3} \tag{27}$$

where d is the diameter of an aerosol droplet.

The set of solutions giving possible values for aerosol droplet diameters can be presented in the form

$$d = \frac{1}{\pi} \left(\frac{2\sigma\pi}{\rho f^2} \right)^{1/3} [l(l-1)(l+2)]^{1/3}. \tag{28}$$

On the other hand, in accordance with the vessel geometry (parallelepiped), oscillations characteristic of the liquid itself, which cause the generation of standing waves, can be described by the function that defines the rate potential as [16,18,19]

$$\phi = K\cos(qx)\cos(ry)\cos(sz)\cos(\omega t) \tag{29}$$

where q, r and s are given by

$$q = \frac{m\pi}{a}; \quad r = \frac{n\pi}{b}; \quad s = \frac{p\pi}{h} \tag{30}$$

where a, b and h are the dimensions of the liquid column, and m, n and p are integers showing selected values for the degenerated wave frequency.

Since q, r and s values are chosen to satisfy the condition

$$q^2 + r^2 + s^2 = \frac{\omega_s^2}{c^2} \tag{31}$$

where c is the rate of capillary wave propagation, and ω_s is the corresponding spherical oscillation frequency if the wave knot points are at positions corresponding to $x = 0, a$; $y = 0, b$; $z = 0, h$, it follows that

$$\frac{d\phi}{dx} = 0; \quad \frac{d\phi}{dy} = 0; \quad \frac{d\phi}{dz} = 0 \tag{32}$$

wherefrom

$$\omega_s^2 = c^2 \pi^2 \left(\frac{m^2}{c^2} + \frac{n^2}{b^2} + \frac{p^2}{h^2} \right). \tag{33}$$

If the film thickness is small enough ($h \ll a, b$), then from

$$f = \frac{c}{2} \sqrt{\frac{m^2}{c^2} + \frac{n^2}{b^2} + \frac{p^2}{h^2}} \tag{34}$$

one gets

$$f = \frac{c}{2} \frac{p}{h}. \tag{35}$$

From Eqs. (20) and (35) for resonant frequency (forced frequency of ultrasonic oscillator equal or close enough to the liquid column frequency, i.e. $f = f_s$), we get

$$d = \left(\frac{\pi \sigma}{\rho \dfrac{p^2 c^2}{4h^2}} \right)^{1/3} \tag{36}$$

where p is an integer.

The distribution spectrum is obtained as a series of values

$$d_n = \frac{[2l(l-1)(l+2)]^{1/3}}{\pi} d \tag{37}$$

where d is the value corresponding to the resonance of both liquid column and forced oscillator frequency. The values d_n correspond to a set of resonant liquid column frequencies for different factors of wave shapes, dependent on different damping factors of transverse and longitudinal waves generated by ultrasonic excitation. The minimum frequency obtained from a series of estimated frequencies, due to degeneration of spatial wave shapes (aerosol droplets), can be presented as
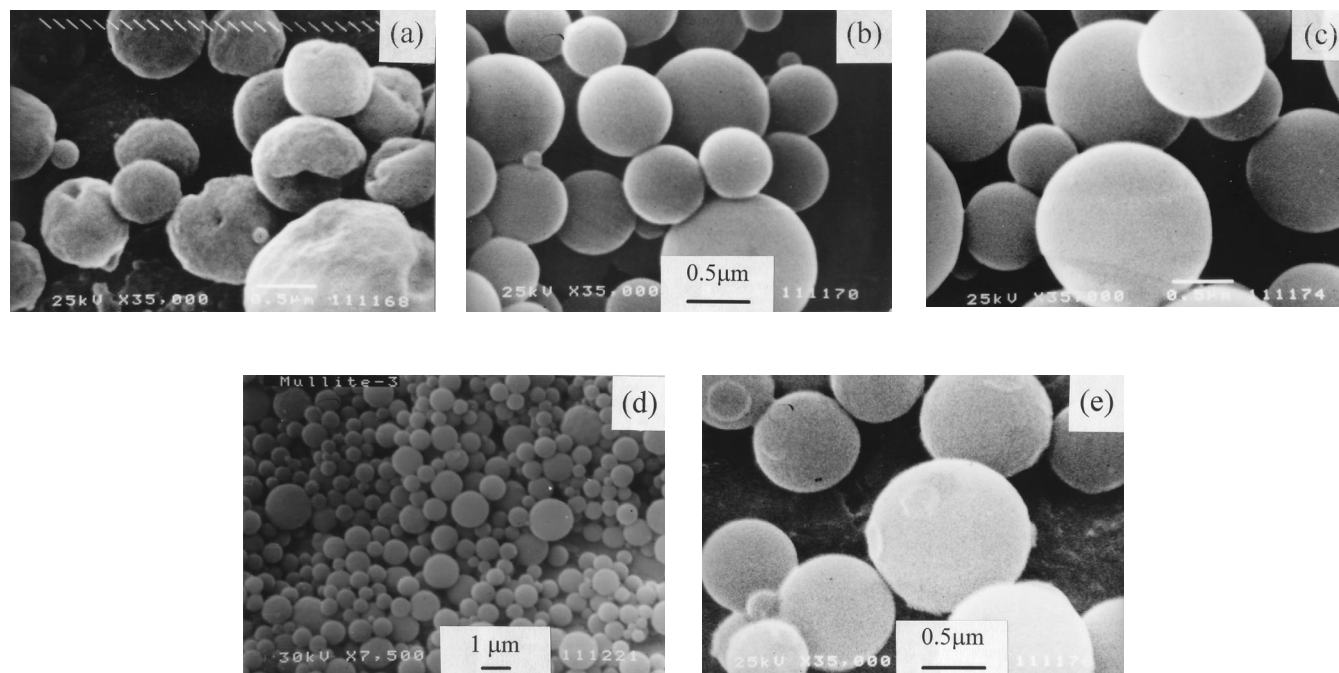

Fig. 2. SEM micrographs of as-sprayed Al$_2$O$_3$, mullite and cordierite powders obtained by the ultrasonic spray pyrolysis: (a) A-1, (b) A-2, (c) M-2, (d) M-3 and (e) C-1 powders.
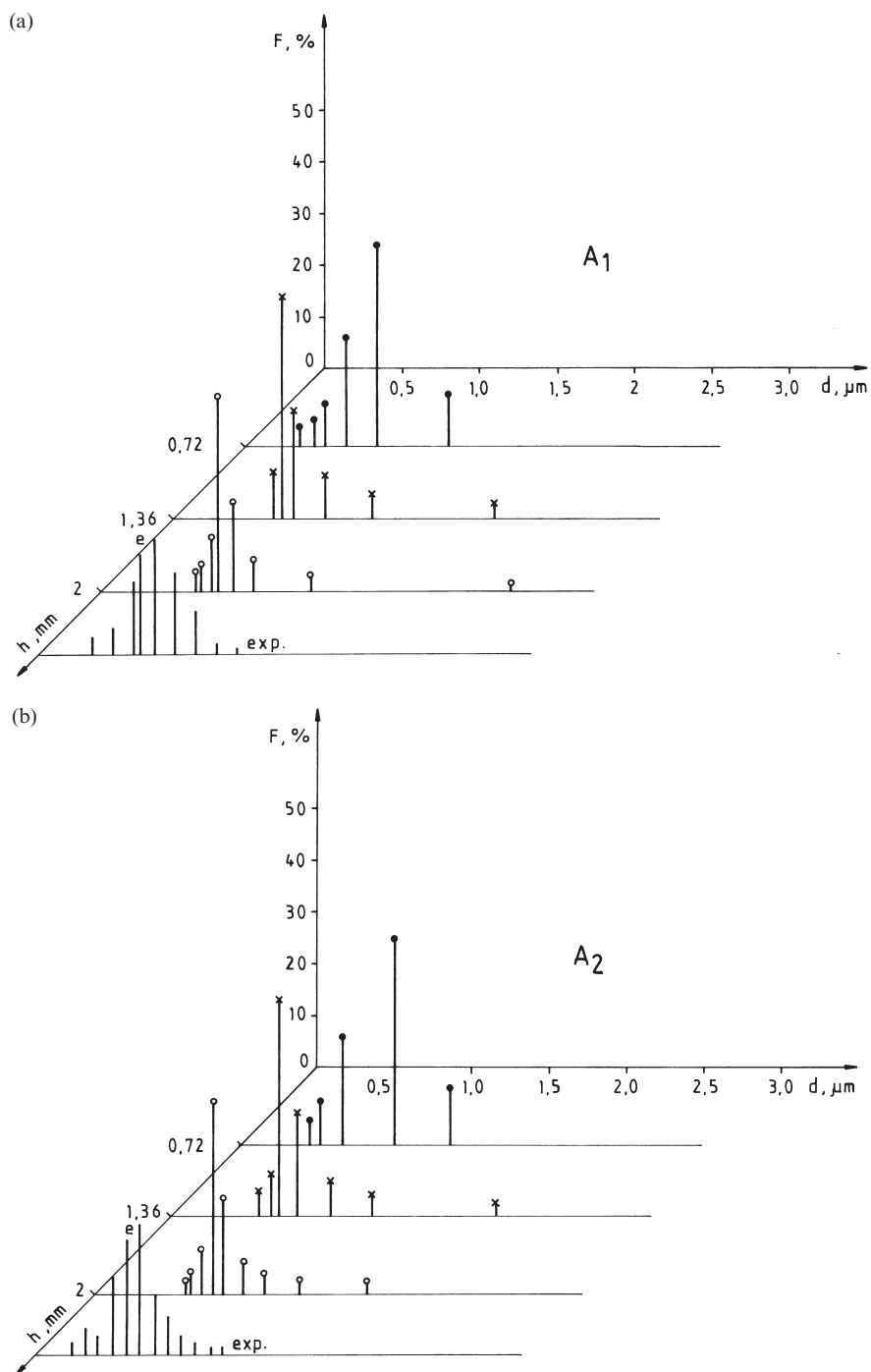
(a)

(b)

Fig. 3. Experimentally determined ($\triangledown$) and theoretically calculated spectrum of particle size distribution of Al_2O_3, mullite and cordierite powders for different liquid column width h: (a) A-1; (b) A-2; (c) M-2; (d) M-3 and (e) C-1 powders; ●, 0.72 mm; ×, 1.36 mm; ○, 2.00 mm.

follows:

$$f_{no} = \frac{2\sqrt[3]{2}}{\pi} f_s \qquad (38)$$

and, accordingly, the aerosol droplet diameter

$$d_{no} = \frac{2\sqrt[3]{2}}{\pi} d \qquad (39)$$

that is

$$d_{no} \approx 0.8d \qquad (40)$$

(for $l=2$) where d is given by Eq. (13), i.e. Eq. (36).

During spray pyrolysis, under the influence of thermal treatment in the furnace, the droplet is transformed into a solid particle the diameter of which could be calculated (assuming that particles are solid) as follows [3,4,10]:
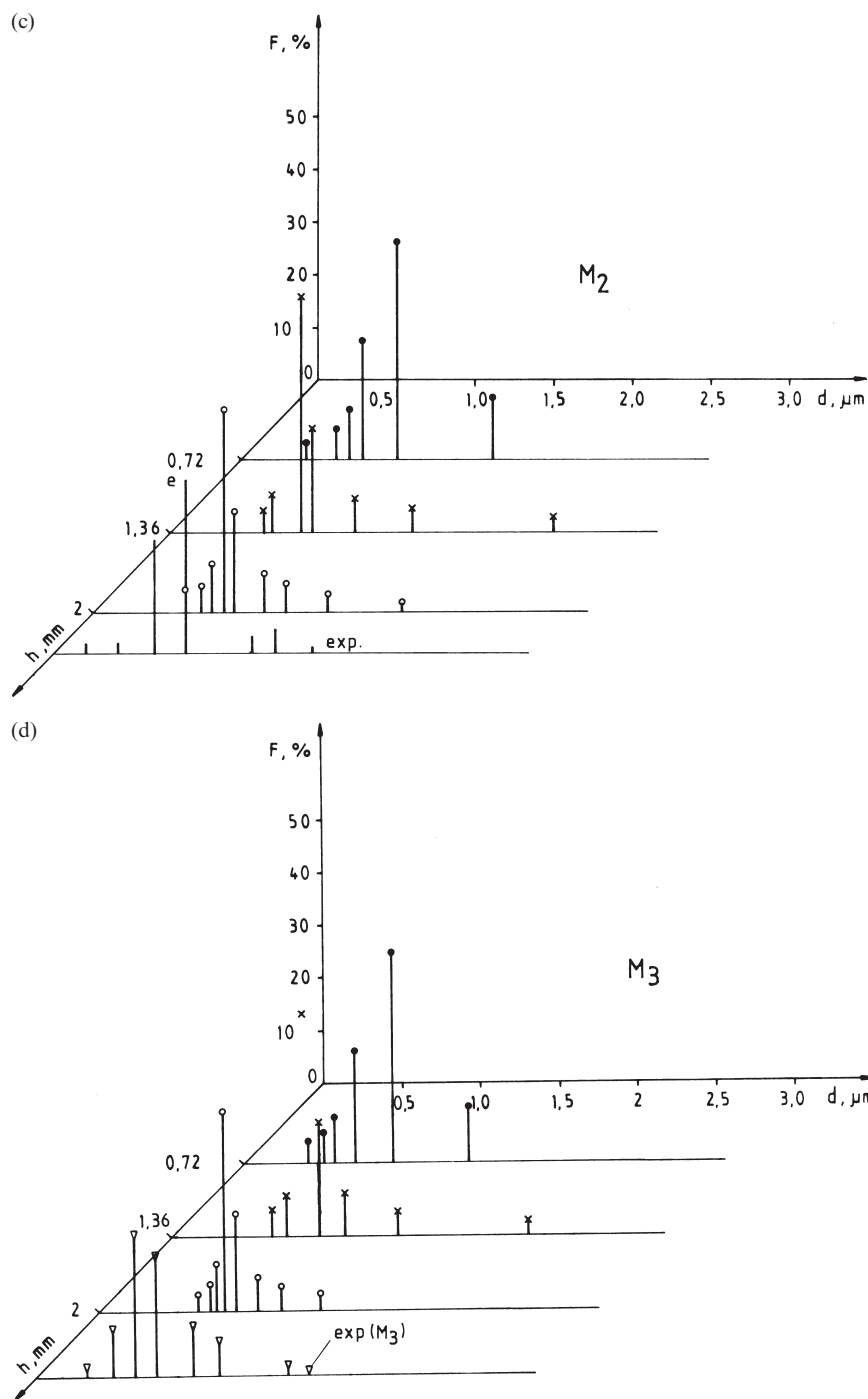
(c)

(d)

Fig. 3. (continued)

$$d_p = d \left(\frac{C_p M_o}{\rho_o M_s} \right)^{1/3} \qquad (41)$$

where d_p is the particle diameter, d is the aerosol droplet diameter, p_o is the oxide density, M_o is the oxide molecular mass, M_s is the starting component molecular mass, C_p is the concentration of precursor used for preparation of the corresponding spray mixture (starting mixture solution for A-1 and A-2 samples, and combina-tions of sols and solutions of different components for M-2, M-3 and C-1 samples as described in Section 2).

4. Results and discussion

SEM micrographs of as-sprayed Al_2O_3 (A-1 and A-2), mullite (M-2 and M-3) and cordierite (C-1) pow-
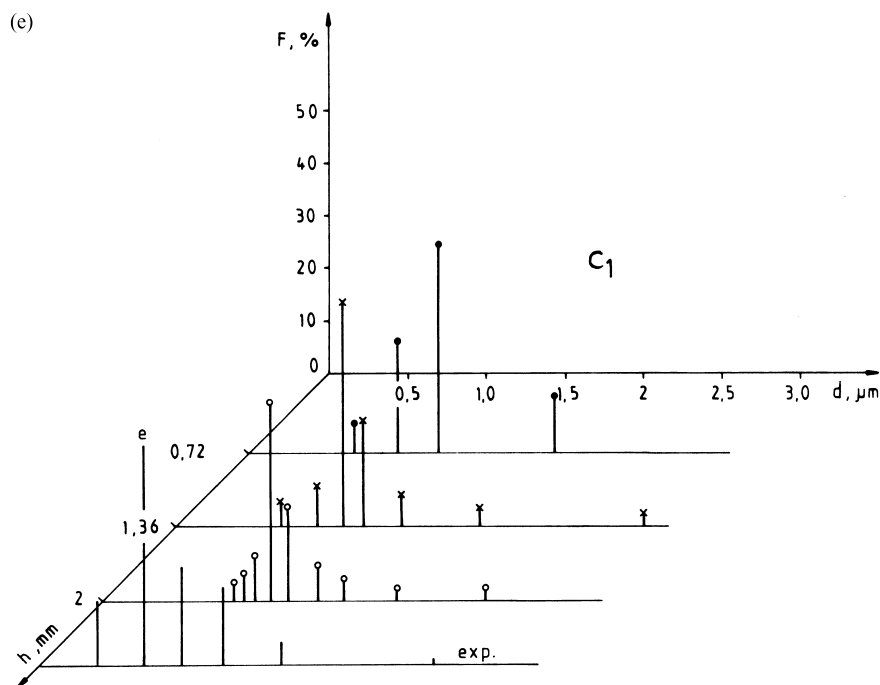
(e)

Fig. 3. (continued)

ders obtained by the ultrasonic spray pyrolysis are presented in Fig. 2. These micrographs show the typical morphology and ceramic particle size distributions of the powders obtained.

The mean particle sizes and distribution of these powders obtained according to the experimental stereological analysis data and the theoretical model were analyzed and the results are presented in Fig. 3.

Despite the difference in the starting systems (phase homogeneity, type of synthesis, chosen starting components, aerosol droplet precipitation mechanism, thermal treatment) [8–11], there are numerous common elements that enable design of the final particle shape and size to be presented as a process determined by harmonization of the forced field exciting the system and the field of the system itself.

On the one hand, the distribution phenomenon considered has been determined by the mean particle sizes, which provides a global insight into the particle size distribution. On the other hand, it has been analyzed via distribution spectra that define particular discrete values obtained by physical fields harmonization. These discrete values represent the products of degeneration of the forced frequency of the ultrasonic oscillator caused either by a change in the standing capillary wave shape (while penetrating the given liquid column) or by generation of a resonant wave field (of the forced oscillator with the liquid column field).

Along with this, the level of resonant harmonization of the forced physical field with the physical field of the system itself was defined by the quality factor Q, which allows prediction of a probability of formation of the given particle size in relation to the total number of particles formed. In this way, the distribution spectrum was determined not only by its discrete values but by their corresponding intensities as well.

4.1. Mean particle size analysis

As the first step in determining the particle size distribution, a comparison was made between the mean particle size values determined experimentally and those estimated theoretically using Eq. (13), Lang's equation and Eq. (41) (Table 1). For the calculation of droplet size according to Eq. (13) and Lang's equation, the following values for surface tension and density are used: $\sigma = 72 \times 10^{-3}$ N/m and $\rho = 1000$ kg/m^3.

Comparison of discrepancies between the experimentally determined and theoretically estimated values shows that the discrepancy when Eq. (13) was used for calculation is in the range from 4 to 16%, whereas in the case of Lang's equation this range is much wider: between 8 and 47.5%. The discrepancy, even for each particular system, is larger when Lang's equation is used, which leads to the conclusion that Eq. (13) more adequately describes the mean particle size for all systems investigated. Studies of some other systems (NiO, Ni, SiC, TiO$_2$) [20–22], not analyzed particularly in this work, show similar conclusions, which makes Eq. (13)

Table 1
Theoretically estimated and experimentally determined mean particle sizes and reduction factor for different systems

	Mean powder particle size (μm)				
	A-1	A-2	M-2	M-3	C-1
Experimental values	0.73	0.64	0.94	0.82	0.91
Calculated values					
Lang's equation	0.52	0.52	0.60	0.57	0.72
Eq. (13)	0.76	0.76	0.89	0.84	1.06
Reduction factor according to Eq. (41)	0.23	0.23	0.27	0.25	0.32

generally more adequate for estimation of the mean particle size than Lang's equation.

Without going into details of this analysis, it is obvious that this fact is significant from the practical point of view as it shows that Eq. (13) offers an adequate alternative to Lang's equation.

4.2. Particle size distribution analysis

Certainly, besides the undeniable importance of such a fact, it is not basically, in relation to the given model as a whole from the qualitative and quantitative points of view, adequate enough to describe the whole particle size distribution spectrum and all its specific qualities.

Because of that, the distribution spectrum has been assumed, in the course of analysis, to be a result of the degeneration of the forced frequency. This degeneration is caused by the change in capillary wave shape and by the harmonization of the forced frequency with the characteristic frequencies of the liquid column inside which the given capillary disturbance is induced. According to Eqs. (28), (36) and (37), the calculated distribution spectrum using Eqs. (28) and (37) is given as

$$d_0 : d_1 : \ldots : d_n = 0.8d_s : 1.24d_s : \ldots : \frac{[2l(l-1)(l+2)]^{1/3}}{\pi} d_s$$

(42)

where l takes on the values in a sequence 2, 3, 4, …, according to the previously given theoretical interpretation.

If this calculated distribution spectrum is compared with the experimentally determined one, then a very good agreement is observed for the conditions where l is limited by the values corresponding to $l=2$ (spherical capillary wave) and $l=3$ (ellipsoidal waves with the least discrepancy from the spherical form).

The reduction of the distribution spectrum to such a narrow range (distribution corresponding to the values $l=2$ and $l=3$), however, cannot provide a complete interpretation of the particle distribution. Namely, two factors as evident from Eqs. (36) and (37), affect the

distribution spectrum: the change in wave shape due to its damping and the change in characteristic frequency of liquid column (induced mechanical oscillator) due to the change in its geometry (width).

The first factor (the change in wave shape) is dominant in the cases of wider liquid columns. A larger width corresponds to higher values of transverse wave damping factor and a higher degree of wave shape degeneration, which incorporating other values of the series, according to Eq. (28), leads to the broadening of distribution spectrum.

The second factor (the change in characteristic frequency of the liquid column) dominates in the case of a small liquid column width (0.76 mm). In this case, during spray pyrolysis a relatively large change occurs in the liquid column width (compared with the initial one). This change in width corresponds to a significant change in characteristic frequency of the liquid column, Eqs. (34) and (35). Therefore, for the case of a very small liquid column width a characteristic widening of distribution spectrum takes place.

Accordingly, these two factors are obviously the basic harmonization (selection) factors of distribution. Although they always act together, which one of them will dominate evidently depends on the relative change in the liquid column width.

Upon analyzing the experimentally obtained distribution spectra for mullite (M-2 and M-3) and particularly cordierite (C-1), it can be seen that the lines in the particle distribution spectra of these systems are shifted toward higher values of particle diameters when compared with the lines of the Al_2O_3 (A-1 and A-2) spectrum. Additionally, a wider range of particle distribution corresponds to these spectra (Fig. 3). This can be ascribed to the differences in concentrations of precursors used and the specific properties of the starting components, as well as to the mass of the final phases constituting the powder particles after their complete consolidation via precipitation, drying, pyrolysis and sintering, according to Eq. (41).

The specific characteristics of the particle size distribution spectrum (compared with those of the aerosol

droplet distribution) basically arose from different reduction factors, i.e. different starting component concentrations and their molecular masses, as well as from the molecular mass and density of phases formed in the system at the end of the process. They are not connected with the degeneration of the forced oscillator field frequency during deformation transport through the given liquid column, and, as such, they represent reduced forms of already formed discrete values, at the aerosol droplet level.

The spectrum width and the determined quantitative values of some powder particles' discrete values are determined by the aerosol droplet distribution spectrum, which is of primary importance for particle formation. To obtain a final quantitative particle size value it is necessary to incorporate the factor of aerosol droplet volume reduction during solidification. This is important for determination of the quantitative values of the spectrum, which from the point of view of particle formation is of less importance.

If the probability of appearance of the given discrete value for particle size in the distribution spectrum is considered to be equivalent to the resonant wave amplitude Y_r, then according to

$$Y_p = \frac{H}{2\beta m_o \Delta\omega} = \frac{H}{4\pi\beta m_o \Delta f} \tag{43}$$

where Y_p is the amplitude of resonant wave, H is the forced force, β is the factor of environment resistance, m_o is the oscillator mass, and Δf is the difference between the forced frequency of the ultrasonic oscillator and the characteristic frequency of the liquid column.

Assuming that $H/4\beta m$ has approximately the same value for different aerosol droplets, then we get

$$Y_{01} : Y_{02} : \ldots : Y_{0n} = \frac{1}{\Delta f_1} : \frac{1}{\Delta f_2} : \ldots : \frac{1}{\Delta f_n} \tag{44}$$

from which the relationship between the corresponding wave amplitudes (which in our case is equivalent to the frequency of appearance of the given discrete value for a particular particle size in the spectrum to the total number of particles formed previously normed as fraction 1 or 100%, if the frequency appearance is given in percent), can be expressed as the ratio of reciprocal values of differences of forced to degenerated frequencies. This gave diagrams $F = \phi(d)$ (ϕ stands for the function) which define quantitatively the whole spectrum (Fig. 3).

In considering specific characteristics of the system it has been already said that a smaller width of liquid column h corresponds to wider spectra, the maxima of which are shifted towards higher droplet diameter values, thus making the spectra asymmetric (Fig. 3).

The harmonization of physical fields via the quality factor Q

$$Q = \frac{f_s}{4\pi\Delta f} \tag{45}$$

where f_s is the characteristic frequency of the liquid column as an oscillator and Δf is the difference between the forced and characteristic of the system frequency or via the parameter of the half-width of the resonant curve

$$\Delta f = \frac{f_s}{4\pi Q} \tag{46}$$

gives similar results.

With increasing film thickness, the characteristic frequency of the liquid column will approach the forced frequency of the ultrasonic generator if the degenerated frequencies with maximum frequencies of appearance only (those corresponding to approximately 80% of the total number of particles) are taken into account. This is evident from Fig. 4, which shows the maximum distance between the degenerated and forced frequency dependence on the liquid column depth. Accordingly, an increase in film thickness causes an adequate increase in the quality factor (Fig. 5).

A detailed presentation of the harmonization degree of physical fields and its influence on the spectrum generation is illustrated in Fig. 6 as the quality factor dependence of the frequency shift in the whole spectrum versus the forced frequency for different film thicknesses. It can be seen that the resonant maxima are nearer to the forced frequency if the liquid column width is larger.
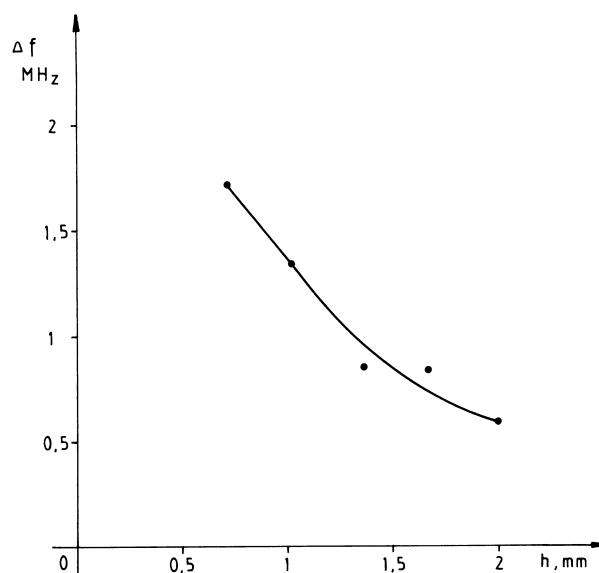

Fig. 4. Dependence of difference between the forced and characteristic system frequency Δf on the liquid column width h.
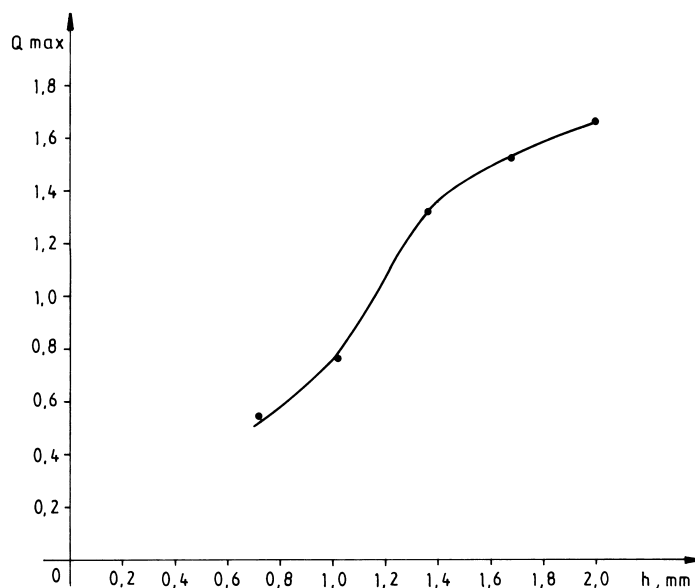
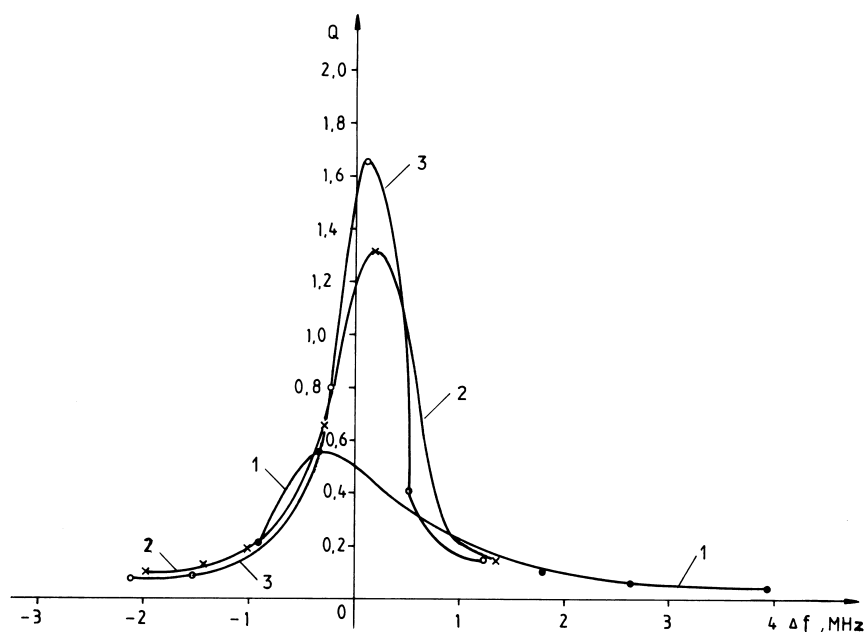Fig. 5. Dependence of the quality factor Q on the liquid column width h.

Fig. 6. The quality factor Q dependence on the frequency shift from the forced frequency for different liquid column widths: (1) 0.72 mm; (2) 1.32 mm; (3) 2.00 mm.

Also, it is evident that a smaller width of the liquid column corresponds to a wider spectrum.

The spectra for mullite and especially cordierite powders are somewhat broader due to the volume reduction factor acting during transformation of aerosol droplets into powder particles. Hence, the values corresponding to the maximum frequencies of appearance of particles of uniform size are lower.

5. Conclusions

The distribution spectrum is completely determined by the degeneration of the forced frequency of the ultrasonic oscillator conditioned by the change in the standing capillary wave shape in relation to an ideal spherical one and by the factor of resonant harmonization of that frequency with the characteristic frequency

of the liquid column, which is also an induced oscillator.

The frequency of appearance of a particular discrete value for particle size, derived as an equivalent to the resonant wave amplitude, enabled the definition of not only discrete values inside the given distribution but their probability of appearance as well, determining in this way the given spectrum via the intensities of its lines.

The distribution spectrum has been analyzed in detail (including values of particular discrete quantities, frequency – intensity of its appearance, quality factor, and half-width of resonant peak) for each selected system (Al$_2$O$_3$: A-1 and A-2; mullite: M-2 and M3; cordierite: C-1) and the agreement between theoretical and experimental values is shown.

A high level of agreement of the given values enabled a better interpretation of the process of particle genesis in which the phenomenon of resonant harmonization of physical fields of an ultrasonic oscillator and a liquid column exposed to its action plays a dominant role.

Appendix A

All the systems studied in this work are low-viscosity ones. Therefore, it is possible to interpret in a similar way the genesis of powder particles of all low-viscosity system by ultrasonic atomization.

The interpretation of high viscosity systems (solidification of metals and glasses, estimation of particle sizes formed during solidification in high ultrasonic field frequency acting on the system and vice versa, estimation of frequency intensity necessary for solidification of the melt to obtain very fine solidified system structure) is rather complex and owing to its significance it has been particularly treated.

For the condition where the oscillation amplitude is small, compared with the liquid column depth for viscous systems with low/high coefficient of capillary wave decrease, the potential rate can be expressed as

$$\phi_x = e^{-i\omega t + ikx}(A\,e^{kh} + B\,e^{mh}) \tag{A1}$$

$$\phi_h = e^{-i\omega t + ikx}(-iA\,e^{kh} - iB\,e^{mh}) \tag{A2}$$

and

$$\frac{p}{\rho} = e^{-i\omega t + ikh}\frac{\omega}{k}A\,e^{kh} - gh \tag{A3}$$

where

$$m = \sqrt{k^2 - \frac{i\omega}{\eta}}. \tag{A4}$$

Here k is the wave vector, ω is the spherical oscillation frequency of the ultrasonic oscillator, η is the viscosity coefficient, and A and B are harmonization constants.

For a low damping wave coefficient (low viscosity systems)

$$\eta k^2 \ll \sqrt{gk} \tag{A5}$$

the relation between spherical frequency and viscosity can be written in the form

$$\omega = \pm\sqrt{gk} - 2i\eta k^2 \tag{A6}$$

where i is the imaginary unit.

For the case of high viscosity (high viscosity systems),

$$\eta k^2 \gg \sqrt{gk}, \tag{A7}$$

the real solution of the equation for the corresponding capillary wave can be described as

$$\omega = \eta k^2 \tag{A8}$$

for extremely amortized oscillations.

Bearing in mind that $k = \pi/d$, it follows that

$$f = \frac{\eta\pi}{2d^2}, \tag{A9}$$

implying

$$d = \left(\frac{\eta\pi}{2f}\right)^{1/2}. \tag{A10}$$

The wave generated inside the liquid column can be described by Mathieu's functions:

$$\frac{d^2y}{dt^2} + 4\eta\frac{k^2}{\rho}\frac{dy}{dt} + \left[\frac{\sigma h^3}{\rho}\text{th}(kh) - kg\text{th}(kh)\right]y = 0 \tag{A11}$$

and the change in wave amplitude with time as

$$y(\tau) = \exp\left[\left(\mu - \frac{2\eta h^2}{\rho}\omega_o\right)\tau\right]p(\tau) \tag{A12}$$

where $p(\tau)$ is a periodic function dependent on time τ, and μ is a factor dependent on τ, ρ, ω_o and k.

References

[1] K.S. Suslick, MRS Bull. 4 (1995) 29.
[2] R.J. Lang, J. Acoust. Soc. Am. 34 (1) (1962) 6.
[3] G.L. Messing, S.C. Zhang, G.V. Jayanthi, J. Am. Ceram. Soc. 76 (1993) 2707.
[4] G.W. Jayanthi, S.C. Zhang, G.L. Messing, Aerosol Sci. Technol. 19 (1993) 478.
[5] T.Q. Lin, O. Sakurai, N. Mizutami, M. Kato, J. Mater. Sci. 21 (1986) 3698.
[6] M. Ocana, J. Sanz, T. Gonzales-Carreno, C.J. Serna, J. Am. Ceram. Soc. 76 (1993) 2812.
[7] K. Moore, J. Cesareno III, D.M. Smith, T.T. Kodas, J. Am. Ceram. Soc. 75 (1992) 213.
[8] V. Jokanović, Dj. Janaković, A.M. Spasić, D. Uskoković, Mater. Trans. JIM 37 (1996) 627.

[9] D. Janaković, Lj. Kostić-Gvozdenović, Lj. Živković, D. Usko-ković, J. Mater. Res. 11 (1996) 1706.

[10] Dj. Janaćković, V. Jokanović, Lj. Kostić-Gvozdenović, D. Usko-ković, Nanostruct. Mater. 10 (1998) 341.

[11] Dj. Janaćković, V. Jokanović, Lj. Kostić-Gvozdenović, S. Zec, D. Uskoković, J. Mater. Sci. 32 (1997) 163.

[12] A.M. Spasić, V. Jokanović, J. Colloid Interface Sci. 170 (1995) 229.

[13] A.M. Spasić, V. Jokanović, D. Krstić, J. Colloid Interface Sci. 186 (1997) 434.

[14] V.G. Levič, Fizikohimijčeskaja Hidrodinamika, AN SSSR, Moscow, 1952.

[15] N.W. McLachlan, Theory and Applications of Mathieu Func-tions, Oxford University Press, London, 1947.

[16] K.F. Herzfeld, T.V. Litovitz, Absorption and Dispersion of Ultra-sonic Waves, Academic Press, New York, 1959.

[17] E.U. Condou, H. Odiskaw, Handbook of Physics, McGraw-Hill, New York, 1958.

[18] L.D. Landau, E.M. Lifšic, Mehanika Neprekidnie Sredi, AN SSSR, Moscow, 1960.

[19] J.J. Harmans, Flow Properties of Disperse Systems, North-Holland, Amsterdam, 1953.

[20] S. Stopić, I. Ilić, D. Uskoković, Mater. Lett. 24 (1995) 369.

[21] Lj.S. Čerović, S. Milonjić, Lj. Živković, D. Uskoković, J. Am. Ceram. Soc. 79 (1996) 2215.

[22] J. Nedeljković, Z. Šaponjić, Z. Rakočević, V. Jokanović, D. Usko-ković, Nanostruct. Mater. 9 (1997) 125.